Singlet-exciton transport and spatial and energetic disorder in dibenzofuran crystals

U. Fischer, C. von Borczyskowski, and N. Schwentner
Institut für Experimentalphysik, Freie Universität, Berlin, Arnimallee 14, D-1000 Berlin 33, Federal Republic of Germany
(Received 21 June 1989; revised manuscript received 5 December 1989)

The trap-depth distribution of dibenzofuran singlet excitons and the temperature-dependent energy migration and energy transfer to anthracene super traps has been studied by time-resolved spectroscopy via synchrotron radiation and two-photon laser excitation. The energy transport in the orientationally disordered dibenzofuran single crystals follows a stretched exponential behavior with $\beta=0.57$ at temperatures above 150 K. Below this temperature β approaches zero. Spatial (fractal) disorder has been experimentally separated from energetic (temporal) disorder by applying the subordination principle. Spatial disorder indicates an aggregation of orientationally disordered molecules. The aggregates are described by the spectral (fracton) dimension $d_s=1.14$ over the characteristic diffusion length.

I. INTRODUCTION

Aggregation processes in disordered media are often described by the concept of fractal structure.[1] This approach may be very evident, e.g., for diffusion-limited cluster aggregation in aerosols and colloids.[2] Less evident, however, are aggregationlike phenomena during the solidification process of crystalline phases with structural disorder caused by lattice defects or static orientational fluctuations.[3] Dynamic processes such as electric conductivity and excitation energy transport will be very sensitive to aggregation since they critically depend on the geometric nature of the underlying lattice.[4] They are well-suited tools to explore the details of the spatial structure. Due to the immanent geometric and/or energetic disorder, for example, in polymers, glasses, and binary random crystal lattices, kinetics often become dispersive.[5] A discrimination between geometric and energetic contributions is very attractive, since it might be possible to determine the effective (spatial) dimension of the disordered lattice.

Several theoretical[6,7] and experimental[8,9] attempts have been reported to unravel these two effects. Spatial disorder, in which we are interested with respect to aggregation processes, might be characterized via a fractal dimension $\bar{d}$, whereas temporal disorder will result in a waiting-time distribution.[10] Temporal disorder often arises due to energetic disorder.[6,9] As a consequence, energetic disorder, and thus the waiting-time distribution will depend on temperature, which provides experimental means to separate both kinds of disorder. Recently, this has been successfully applied to percolating clusters at criticality[9] making use of the subordination principle.[6] This principle states that in the continuous-time random-walk (CTRW) situation the spectral dimension d_s combines (for $d_s<2$) with the parameter $0<\gamma<1$ of a waiting-time distribution $\psi(t)\sim t^{-1-\gamma}$ to an effective spectral dimension $d_e=\gamma d_s$.[6] Temperature-dependent aspects of this subordination have recently been investigated by computer simulations also.[7]

The progress in this field encourages investigations on more complicated systems, where the relation of these two types of disorder are not known from the beginning. One class of such systems are molecular crystals formed from noncentrosymmetric molecules, which often show orientational disorder.[3] We report on energy transport in the optically excited lowest singlet state of the organic molecular crystal dibenzofuran (DBF). From x-ray structure analysis it is known[11] that about 9% of the molecules are rotated by 180° along the long in-plane axis as compared to the bulk molecules. This is shown schematically for the a-b plane of the crystal (Fig. 1). As is immediately evident, this will result in orientational (that is geometric) disorder of the crystal lattice. As has already been shown for other orientationally disordered crystals[12,13] strong influence on the energy distribution of excited states as well as the energy transport kinetics are expected.

The energy distributions of the singlet-exciton trap states of DBF are reinvestigated in Sec. III A to clarify a discrepancy between the existing one-photon spectra[14–16] and a two-photon spectrum.[17] The intrinsic nature and the origin of the energy distribution are discussed in detail. The quantum efficiency of the energy transfer of the DBF excitons to anthracene is reported in Sec. III B for a large range of concentrations (2–1700 ppm) and temperatures (5–300 K). The data indicate a sequential energy transfer due to a migration in the DBF trap states and a subsequent transfer to the anthracene super traps. The dispersive nature of the energy transfer follows from the time dependence of the fluorescence (Sec. III C) and a strongly temperature-dependent stretched exponential parameter β is extracted from the data. The spectral dimension d_s of the orientational disordered aggregates will be derived from the high-temperature limit of β in the discussion (Sec. IV). The temperature dependence of β is attributed to a waiting-time distribution.

A similar experimental study has been carried out by Hoffmann[18] with a qualitative description of the transfer rates. Our spectroscopic results agree quite well with

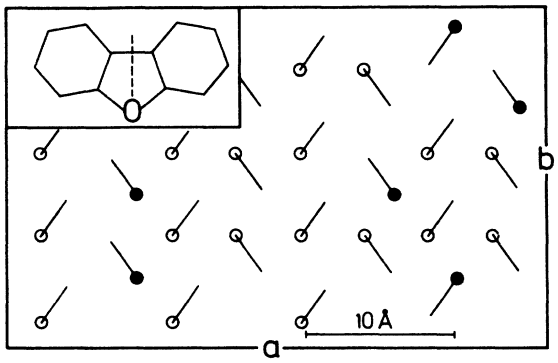

FIG. 1. Crystallographic a-b plane of dibenzofuran (DBF). The intersection of the DBF molecule with this plane is indicated in the inset. The orientational disorder is shown schematically.

those of Hoffmann but the time courses for the transfer differ significantly. Especially the lifetimes in the 15- and 60-ns regime are not reproduced by our data. Therefore, our attempts of a quantitative description also yield a different picture concerning the transfer by trap states and exciton-band states. The present investigations have also been motivated by the fading observed in the DBF and anthracene fluorescence in triplet exciton-transport experiments.[19]

II. EXPERIMENT

DBF has been synthesized in order to avoid impurities present in technical grade material.[14] Single crystals have been grown from the melt by standard Bridgeman techniques after extensive zone refining and doping with purified anthracene. The crystals show a concentration gradient in radial and axial directions and have been cut into pieces of $3\times2\times1$ mm^3 size. The actual anthracene concentration has been determined by liquid-phase chromatography in n-heptane solution down to anthracene concentrations of 100 ppm. Lower concentrations have been derived from an extrapolation of the ratio of guest to host fluorescence quantum efficiency yielding an accuracy of about 10%.

The energy distribution of trap states in the bulk of the pure crystals has been studied by two-photon absorption to discriminate against possible defects near the surface. For this purpose the crystals have been immersed into a combined bath-flow cryostat (Oxford SMD 8) with the c axis parallel to the wave vector of the exciting light. A dye laser (Fl 2000, Lambda Physics) with rhodamin B pumped by an excimer laser (EMG100, Lambda Physics) has been used for two-photon excitation. The dye laser output has been frequency doubled by a potassium-dihydrogen-phosphate (KDP) crystal for the one-photon spectra. The DBF fluorescence has been recorded by a 1-m Ebert monochromator and a Valvo XP 2020 Q photomoltiplier. The spectra have been averaged in a multichannel analyzer and transferred to a PDP 11 computer for further evaluation. The synchrotron radiation of BESSY has been used for the more surface-sensitive one-photon spectra of pure crystals and especially for studying the time dependence of the energy transfer in the doped samples thus exploiting the favorable time structure. The light is dispersed by a 3-m monochromator with an ultimate resolution of 0.007 nm in a usable range from 30 to 400 nm and focused onto the sample in a spot of 1.5×0.2 mm^2. The beam line is optimized by collecting mirrors for a high flux.[20] The fluorescence from the sample has been dispersed by a 0.25-m Ebert monochromator with an ultimate resolution of 0.3 nm in the range from 200 to 1000 nm and has been recorded by a three-stage channel plate detector. The light from BESSY is pulsed with a repetition time of 208 ns. The time delays between reference pulses of BESSY and the signal are stored via a time-to-amplitude converter in a multichannel analyzer. The time resolution of the source combined with the detection system corresponds to a FWHM of 700 ps.

III. RESULTS

First the intrinsic nature of the trap states, as well as the influence of excitation conditions and sample geometry on excitation and fluorescence spectra, will be discussed. Next the migration in the trap states is analyzed by the quantum efficiency and the time dependence of the energy transfer to the anthracene supertraps.

A. Trap states of pure dibenzofuran crystals

The energies of the transitions above the zero-phonon line (ZPL) of the exciton band at 32 877 cm^{-1} in our two-photon excitation spectrum at 4.2 K shown in Fig. 2(a), agree with those of the two-photon spectrum in Ref. 17 within 20 cm^{-1}. In the following we will focus our attention to the region below the ZPL. Figure 2(a) shows,

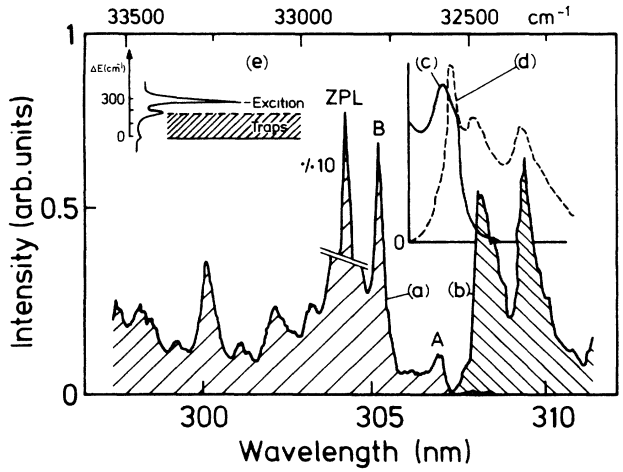

FIG. 2. (a) Two-photon excitation spectrum of the 31 534-cm^{-1} emission band at 4.2 K with the trap bands A and B and the zero-phonon line (ZPL) of the exciton band of a 1-mm-thick single crystal. (b) Corresponding high-energetic part of the fluorescence. (c) Synchrotron one-photon excitation spectrum of the 31 534 emission band of a different about 1-mm-thick single crystal at 6 K. (d) Emission spectrum for one-photon excitation. (e) Schematic trap distribution and exciton ZPL.

on a broad underlying background two pronounced bands A and B at 32 574 and 32 786 cm^{-1} corresponding to depths below the ZPL of 303 and 91 cm^{-1}, respectively. These structures are missing in the two-photon spectra of Ref. 17 but they are similar to absorption lines observed in the one-photon absorption spectrum,[15] which are situated 257 and 89 cm^{-1} below the exciton band. Thus, the new two-photon excitation spectrum confirms the one-photon spectra concerning the lines below the ZPL in general. However, the values for the A bands scatter from 303 cm^{-1} [this work, Fig. 2(a)] down to 257 cm^{-1} (Ref. 15) and up to 352 cm^{-1} from previous one-photon spectra.[14] Therefore, we continued our study by new one-photon excitation spectra of DBF using the synchrotron radiation of BESSY. We focused our attention to the region of the origin of the A state [Fig. 2(c)]. The red wing in the new one-photon excitation spectrum [Fig. 2(c)] coincides with the first maximum of the former one-photon excitation spectrum[14] and reaches a maximum around a trap depth of about 283 cm^{-1}. The band at the highest energy in an emission spectrum taken on the same crystal [Fig. 2(d)] relates to a trap depth of 333 cm^{-1} and overlaps with the wing of the absorption band of Fig. 2(c). This band is missing in an emission spectrum obtained by two-photon excitation [Fig. 2(b)].

These features observed for several samples are characteristic for the way of excitation and can be attributed to the different penetration depths of the light for one- and two-photon excitation spectra. Our crystals, with a thickness of about 1 mm, are rather transparent for two-photon excitation and the resulting excitation spectrum [Fig. 2(a)] displays essentially the energy distribution of states provided there are no strong selection rules involved. The light penetration depth in the case of one-photon excitation is small and thus shows a large variation in the case of thick samples. The one-photon absorption spectra of Ref. 15, however, have been taken from sublimation flakes and meltgrown films between two silica discs (thicknesses 0.1–1.59 μm) to avoid saturation. The energy of the B band is in good agreement with all our results but the energies for A-type lines differ by about ± 50 cm^{-1} as compared to our two-photon excitation spectra. Obviously, this distribution of energies of A-type lines is weighted by the ways of excitation somewhat differently. Also, the different sample preparation, polarization conditions, and a nonuniformity of thickness in the one-photon spectra can play a role. For this reason the two-photon excitation spectra are presumably closest to the actual energy distribution of which we assume is due to different trap states.

The one-photon excitation spectra originate from samples of about 1-mm [Fig. 2(c)] and 5-mm (Ref. 14) thickness. Therefore, the absorption is saturated near the maxima of the trap distributions and the spectra are sensitive to the onset of absorption in the red wing of the trap distribution. The thicker samples of Ref. 14 reach saturation already in the low-density far red wing whereas the thinner sample [Fig. 2(c)] emphasizes the intermediate part of the wing. However, the small penetration depth for one-photon absorption reduces reabsorption of resonantly emitted light. The high-energy band in the emission spectrum [Fig. 2(d)] after one-photon excitation indeed overlaps with the red wings of the trap distributions seen in the one-photon excitation spectrum [Fig. 2(c)] indicating that a narrow distribution of trap states in the bottom of the total A trap distribution is responsible for the emission spectra. The maximum in emission at 32 544 cm^{-1} therefore represents a distribution of trap ZPL in emission without any Stokes shift.

The exciton ZPL in the two-photon excitation spectra is inhomogeneously broadened with an approximately Gaussian line shape and a FWHM of 20 cm^{-1}. The FWHM of the ZPL increases only moderately in the low-temperature range from 20 cm^{-1} at 1.2 K to 30 cm^{-1} at 30 K. At high temperatures most of the structures are smeared out and the ZPL broadens to 100 cm^{-1}. The A and B bands have, at 1.2 K, a FWHM of 30 and 15 cm^{-1}, respectively.

The broad distribution of trap states is also evident from emission spectra after two-photon excitation. The homogeneous excitation of the bulk of the crystals in the case of a two-photon process leads to strong reabsorption of resonance radiation and consequently the trap ZPL at 32 544 cm^{-1} is bleached in the emission for this case [Fig. 2(b)] down to energies corresponding to the far red wing in the trap distribution.

All fluorescence lines shift to the blue by about 30 cm^{-1} when increasing the temperature from 1.2 to 30 K. This indicates that there is a distribution of trap states, of which relative emission intensities depend on temperature. Above 30 K the line positions are stationary and broaden. The zero-phonon lines of the A states exhibit an increasing self-absorption. We tried to verify the assignment to emission from free excitons of the bands indicated by arrows in Fig. 1 of Ref. 18 by a temperature study of highly resolved emission spectra. We can identify the bands marked in Ref. 18 in a low-temperature spectrum at 4.2 K. There is no increase observed by us in the relative intensity of these bands with increasing temperature. The bands are lost around 80–90 K in a background from the broadened, more intense, neighboring trap bands. The bands marked in Ref. 18 in the 200-K spectrum belong to strong trap bands which are situated at somewhat longer wavelengths in the low-temperature spectra. The wrong assignment in Ref. 18 can be caused by the overall blue shift of the emission spectra with temperature by 30 cm^{-1} which has been mentioned above. Therefore, there is no indication of emission from free-exciton bands in our spectra.

States below the ZPL of the unperturbed exciton band could be due to a distortion of the crystals near the surface if they would show up only in one-photon absorption or excitation spectra because of the small penetration depth of the light in this case. The appearance also in the two-photon spectrum of Fig. 2 with an overall intensity similar to that in the one-photon spectrum proves that this absorption is an inherent property of the bulk single crystal. Only the relative intensities of the bands themselves are different in one (Ref. 15) and two-photon spectra which can be an indication of a larger disorder near the surface of the crystal or of a too thick sample for the one-photon experiment.

Once we have established by two-photon excitation that at least the majority of trap states does not belong to surface defects, we would like to discuss the nature of these traps. The two pronounced excitation origins A and B (Fig. 2) below the lowest exciton band of DBF suggest two types of traps related to weakly and strongly distorted molecules according to their trap depth. The deep traps are most likely those molecules which have been identified by x-ray analysis[11] and which are rotated by 180°. The shallow traps B can be tentatively assigned to molecules surrounding a rotated molecule as nearest neighbors. The intensity ratio of about 1:4 for the integrated line intensity of A to B is consistent with this assumption because several surrounding molecules may be distorted by one tilted molecule. It is interesting to note that in the c,b plane with the highest packing of molecules, six molecules would be closest to one rotated DFB molecule. The percentage of rotated DFB molecules of 9% determined by x-ray analysis also agrees approximately with the relative integrated intensities (0.05) of trap A to the ZPL of the exciton band. The broader linewidth of A traps as compared to B traps is probably due to the effect that at trap concentrations larger than 1%, the formation of aggregates (such as "dimers," "trimers," etc.) has to be taken into account, which will certainly result in additional absorption origins or at least in line broadening. Recently, it has been shown for a mixed crystal[21] that the optical transition of a defect site nearest to a doped molecule is not very sensitive to the kind of aggregates responsible for this distortion. Most likely, B traps in DBF show the same behavior. An alternative assignment of maximum B to a vibrational side band of A suggested by the spacing of 212 cm^{-1} seems to be unlikely. The observed intensity ratio of 4:1 for $B:A$ is much larger than the intensity of the analog vibrational sideband relative to the excitonic ZPL (1:30) and the linewidth of the absorption line B is significantly smaller than that of A. According to the analysis of Bree *et al.*[15] a factor group splitting would also be too small.

For the discussion of the energy transport in the trap states we will use a simplified level scheme shown in Fig. 2(e). The ZPL of the excitons is situated 300 cm^{-1} above the bottom of the traps and the broad distribution of traps extends from 0 up to 200 cm^{-1}.

B. Quantum efficiency of energy transfer

The dynamics of energy transport can be monitored by observing the fluorescence from the DBF traps (donor) when small amounts of energetically very low (acceptor) traps serve as energy sinks. Anthracene (An) has been chosen as acceptor because the An singlet state at 25 900 cm^{-1} lies well below the DBF singlet excitons and thermal detrapping from An to DBF can be excluded. In addition, the An singlet state lies above the DBF triplet excitons (24 552), thus, the An singlet emission can be used as exclusive indicator for the DBF singlet transfer efficiency.

The transfer efficiency from DFB increases as expected with the An concentration [Fig. 3(a)]. The structures in

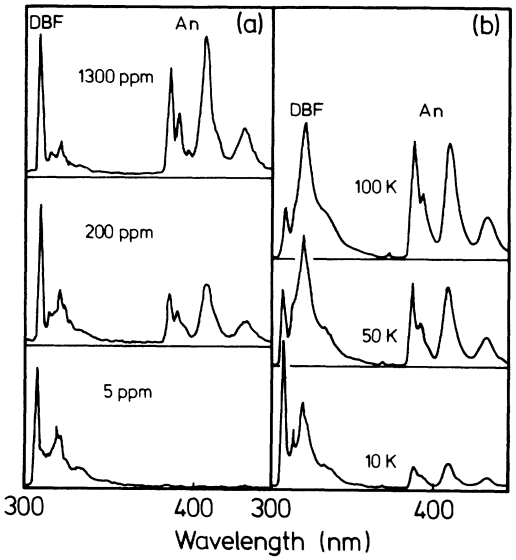

FIG. 3. (a) Concentration and (b) temperature dependence of dibenzofuran and anthracene (An) fluorescence. (a) $T=10$ K, (b) An concentration 30 ppm.

the DBF and An emission spectra agree with literature data.[18,19] The shoulder between 330 and 360 nm is due to a very small carbazol content which could not be completely removed. It has been identified by its excitation and emission spectra and has a lifetime of 15 ns.

The transfer efficiency also rises strongly with increasing temperature [Fig. 3(b)]. This fact demonstrates that we deal with sequential energy transport, i.e., a temperature-dependent migration in the DBF trap states and a subsequent transfer to the acceptor An. The concentration and temperature dependences of the ratio of An quantum efficiency Q_G to DBF quantum efficiency Q_H taken from the integrated emission bands are summarized in Fig. 4.

The emission originates at low temperatures only from the red wing of the A traps independent on the initial excitation energy. This has been checked by excitation into the A and B trap states, into the exciton ZPL, the exciton vibrational sidebands, and into the continuum. Also the

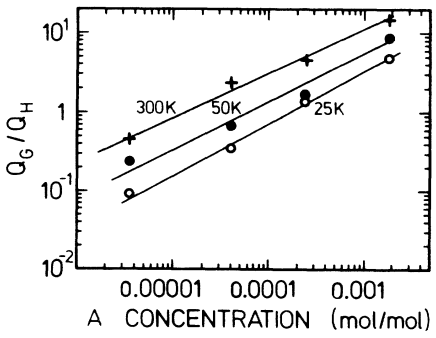

FIG. 4. Ratio Q_G/Q_H of An to DBF integrated quantum efficiencies vs concentration for three temperatures. Solid lines correspond to Eq. (2).

time-resolved data do not depend on excitation energy. The relaxation in the energy distribution of DBF trap states is fast compared to the time scale of energy transfer to An according to these observations. A dispersive migration in the DFB trap states caused by the time distributions for the initial energy relaxation from higher energetic to lower traps as in dimethylnaphtalene[13] is not decisive for the energy transfer in our system within our time resolution.

C. Time dependence of energy transfer

The time course of energy transfer yields more insight into the migration processes in the host traps. Figure 5 shows typical time courses for direct population of the An guest [Fig. 5(a)], for An emission after energy transfer from DFB [Fig. 5(b)], for DBF fluorescence [Fig. 5(c)], and for the stray light [Fig. 5(d)] which displays the experimental time resolution due to the BESSY pulse width and the detection response. The rise of the directly excited guest emission [Fig. 5(a)] and of the host fluorescence [Fig. 5(c)] is prompt in all cases and can be perfectly fitted by the response function [Fig. 5(d)]. The decay in the case of Fig. 5(a) is monoexponential independent on concentration and temperature and corresponds to the radiative lifetime of 1×10^{-8} s for An in DBF. The rise time of An emission for population via energy transfer [Fig. 5(b)] is significantly longer compared to direct population. It can be perfectly fitted for all concentrations and temperatures by using the measured decay of the host as population function. This indicates that the transfer from the host to the guest is direct with no delaying unknown intermediate levels in between. Therefore, the rise of the guest emission contains no additional information and in the following only the decay of the host will be analyzed.

The DBF fluorescence decays are nonexponential and the shape of this nonexponential decay depends strongly on temperature (Fig. 6) and also on An concentration. Despite the single-crystal formation this is not surprising because the orientationally disordered DBF crystal can be regarded as a binary mixture comparable to real two-component compounds.[9] The spatial disorder results in dispersive kinetics due to variations of donor-acceptor separations and/or sequential jumps (on a disordered DBF lattice) before reaching an An trap.

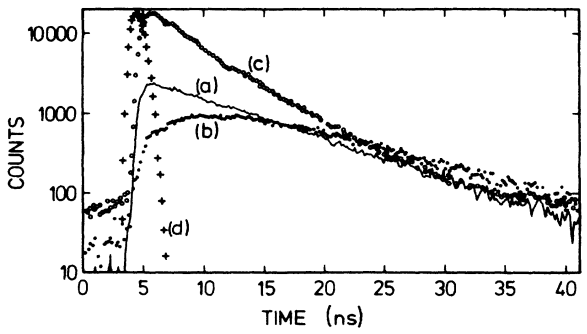

FIG. 5. Time courses of An fluorescence excited directly (a) or via energy transfer from DBF (b), of DBF fluorescence (c), and of the response function (d) from stray light for 5 K and an An concentration of 20 ppm.

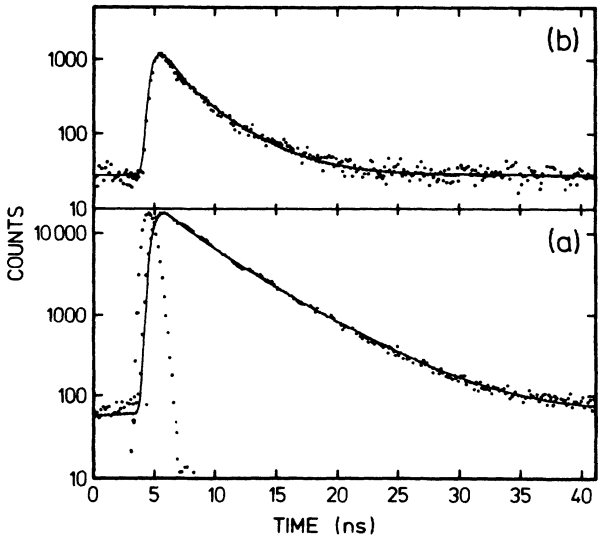

FIG. 6. Decay curves of DBF fluorescence for an An concentration of 2 ppm and temperatures of (a) 5 and (b) 300 K including fits (solid lines) with a stretched exponential. The response function is shown for comparison in the 5-K plot.

Empirically, we could fit (Fig. 6) the fluorescence decay by a Kohlrausch-type[22] stretched exponential behavior over a dynamic range of 2–3 orders of magnitude, where the fluorescence intensity I_{fl} can be expressed as

$$I_{fl}=I_0\exp[-(t/\tau)^{\beta}-t/\tau_0]\ , \tag{1}$$

with $0<\beta<1$ and the singlet lifetime τ_0. It has been checked to see if a biexponential fit would also be appropriate. Biexponential fits result in significant deviations especially at low concentrations. In addition, the transfer quantum efficiencies calculated from the two rates and amplitudes[23,24] are by about an order of magnitude too small compared to the measured quantum efficiencies (Fig. 4) at low concentration and temperature. Only a time-dependent rate constant which increases strongly at short times like that incorporated in the stretched exponential can account for the measured time courses and quantum efficiencies. The radiative lifetime $\tau_0=4.5\pm0.5$ ns of pure DBF is also obtained for the doped crystals. τ is related to a concentration and temperature-dependent transfer time and will not be discussed in more detail. The temperature dependence of β has been derived from fits as in Fig. 6 for all concentrations employed and the results are collected in Fig. 7. No systematic variation of β with the concentration of An has been observed. The β values at lower concentrations are more reliable because the decay curves show a nonexponential behavior over a larger dynamical range. β changes from about zero at the lowest temperature to 0.57 ± 0.09 at 300 K. The strong temperature dependence of β proves the presence of energetic disorder.

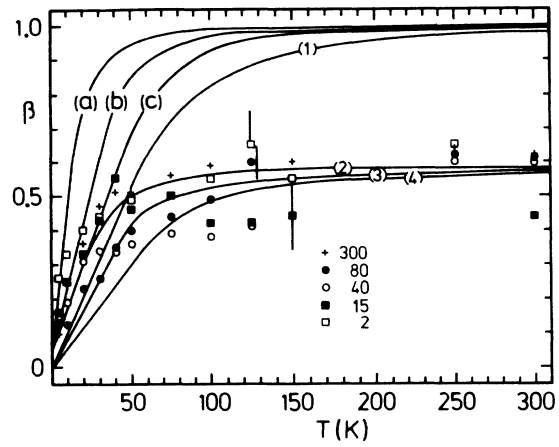

FIG. 7. Experimental points for β as a function of temperature are obtained from fits to a stretched exponential decay with varying concentration of An in ppm. Curves *a*, *b*, and *c* have been calculated according to Ref. 7 assuming $d_s=2$ and $\Delta E=300\ \mathrm{cm}^{-1}$ for an exponential, Gaussian, and uniform distribution, respectively. 1 corresponds to the model of Bässler (Ref. 23) with $\Delta E=300\ \mathrm{cm}^{-1}$. Curves 2, 3, and 4 have been calculated with the Bässler model assuming $\beta=\gamma d_s/2$ and $d_s=1.14$ for energetic distributions of 120, 200, and 300 cm^{-1}, respectively.

IV. DISCUSSION

The DBF trap distributions have been attributed to orientationally disordered molecules and the first shell of surrounding molecules in the bulk of the crystals. The excitation energy migrates in the traps prior to energy transfer according to the temperature dependence of the quantum efficiency. The dispersive nature of the energy transfer is not caused by spectral diffusion because the quantum efficiency and the time courses of the transfer do not depend on the initial excitation energy in the trap distribution. The dynamics of the transport manifest itself in the dispersion parameter β and its temperature dependence. Therefore, the discussion focuses on the contributions of geometric and energetic disorder to the dispersion parameter. An attempt will be made to disentangle these two contributions via the temperature dependence. Assuming a CTRW process[6] for the transport on the disordered DBF lattice the subordination of temporal (energetic) and spatial (fractal) disorder will result in a stretched exponential $\beta=\gamma d_s$.[2] Various models have been proposed to describe the influence of energetic disorder and its dependence on temperature. They all have in common, that for an energy interval ΔE characteristic for the energy disorder γ will approach 1 for thermal energies $kT \gg \Delta E$.

Argyrakis and Kopelman[7] have simulated the temperature dependence for different energy distributions assuming a hopping rate between adjacent sites weighted by $\exp(-\Delta E/kT)$. The result of their calculations is included in Fig. 7 assuming $\Delta E=300\ \mathrm{cm}^{-1}$, which corresponds with the largest energy separation between traps and the exciton band as deduced from the energy distribution shown in Fig. 2. According to this calculation $\gamma \approx 1$ should already be obtained at a temperature close to 100 K.

Assuming only energy disorder, Bässler has suggested for a Gaussian distribution of energies a hopping model, which results in

$$\beta=\gamma=|1+(\Delta E/CkT)^2|^{-1} (C\approx 9)\ ,$$

(Ref. 23) which has been successfully applied for singlet and triplet energy transport in several disordered systems.[13,24] However, it does not describe our experimental results as can be seen in Fig. 7 from a calculation using again $\Delta E=300\ \mathrm{cm}^{-1}$.

Energy disorder may alternatively be incorporated via the concept of hierarchical energy barriers resulting in a description by ultrametric spaces.[6] In this case one would expect γ to increase linearly with temperature as long as $kT \ll \Delta E$ and $\gamma=1$ for $kT \geq \Delta E$.

All the above models claim that γ should approach 1 at thermal energies comparable to a characteristic energy ΔE. This is also evident from a much less sophisticated argument assuming about 10% ($c=0.1$) of DBF molecules energetically 300 cm^{-1} below the exciton band. At temperatures of 300 K the population of excitonic states relative to the one of trap states is

$$\sim[(1-c)/c]\exp(-\Delta E/kT)\approx 2.2\ .$$

This implies that energy transport via the exciton band should be very effective resulting in a purely diffusive energy transport at temperatures above about 150 K.

The observed dispersive transport far above 150 K is in clear contradiction to the expected temperature-dependent change towards $\beta \approx 1$, if assuming only energy disorder or a Boltzmann equilibrium between trap and exciton states. For the given energy distribution of states (Fig. 2), γ should become ≈ 1 above 100 K independent of the anticipated theoretical model (Fig. 7). Consequently, according to the subordination principle from $\beta=\gamma d_s/2$ the spectral dimension can be separated to be $d_s=1.14\pm 0.17$ in the case that $\gamma \approx 1$. In the context of the experimentally known trap to exciton concentration of 1:10 this means that the average number of undistorted lattice sites (exciton states) spatially next neighbored to an excited trap state has to be much less than the predicted value because otherwise we would expect, according to the above arguments, $\beta=1$ at thermal energies covering the energy distribution. This implies that the misoriented DBF molecules related to the traps are spatially closer to each other than expected assuming a statistical distribution. Consequently, orientational disorder does not follow a statistical distribution, but exhibits an aggregation of misaligned molecules. This spatially disordered sublattice is described by a spectral dimension of $d_s=1.14$.

This low value for the spectral dimension indicates a very ramified structure for the distribution of misaligned molecules.[1,4] The discussion of the intensities in the excitation spectra (Sec. III A) showed that the concentration of optically observed traps is close to the concentration of misoriented molecules detected by x-ray spectroscopy.

The optical transition energy of misoriented molecules will differ from that of the bulk material only if the molecules are at least partly surrounded by bulk material and are not placed inside larger homogeneous aggregates of misoriented molecules. The similarity in the concentration of misoriented molecules derived from the optical spectra and the x-ray experiments requires the assumption of a ramified structure for the aggregates of misoriented molecules in agreement with the spectral dimension.

Some estimates can be made about the size of these aggregates. The hopping rate k_h (Ref. 25) is connected with the constant $S=Q_G/Q_H c^p$ in the concentration (c) dependence of the transfer quantum efficiencies Q_G/Q_H of Fig. 4 via

$$k_h=(S/\tau_0)(\eta_H/\eta_G)\ . \tag{2}$$

p is an empirical constant.[25]

A hopping rate of about 1×10^{11} s^{-1} is obtained for 300 K with the radiative lifetime $\tau_0=4.5\times10^{-9}$ s and the ratio $\eta_G/\eta_H=1.4$ (Ref. 26) of the guest to host fluorescence quantum efficiencies. k_h and the nearest-neighbor separation a_0 lead to a mean radial displacement[27] $\bar{r}=(a_0^2\tau_0 k_h)^{1/2}$ of $\sim$120 Å or a diffusion length L of about 70 Å. These displacements are experimental results from the transfer quantum efficiencies down to concentrations which are low enough that the mean separations of anthracene supertraps are larger than the order of L. Therefore, the population in the trap states is able to sample the corresponding volume and the lower length scale of the aggregates has to be at least of this magnitude. We additionally conclude that no microcrystallites of misaligned, but over the diffusion volume well-ordered molecules are formed, since in this case we would observe an exponential relaxation.

The value of $d_s=1.14$ is close to the one of $d_s\approx\frac{4}{3}$ expected independent of the embedding Euclidean dimension for percolating clusters at criticality.[28] Argyakis corrected this value by Monte Carlo simulations for the presence of finite-size clusters additionally to the percolating cluster.[29] For the Euclidean dimensions $d=2$ and 3 he got $d_s'=1.23$ and 1.06, respectively. All values are very close to our experimental result. The critical concentrations for site percolation on squared and cubic lattices are 0.59 and 0.31, respectively.[30] If site percolation applies it follows that the actual concentration of traps within the diffusion sphere is at least three times higher than expected from a pure statistical distribution.

The description of DBF aggregates by percolating clusters is, however, not unique because it does not take the process of aggregation itself into account. On the other hand, fractal dimensions of aggregates have been calculated using models like diffusion-limited aggregation[31] (DLA), cluster-cluster aggregation,[32] and clusters generated by random walks.[33] In the former two cases fractal dimensions of $\bar{d}=1.45$ ($d=2$) (Ref. 31) or $\bar{d}=1.42$ ($d=2$) and $\bar{d}=1.78$ ($d=3$) (Ref. 32) have been calculated. No spectral dimensions have been reported in these cases but, as a general rule, $d_s<\bar{d}$ (Refs. 6 and 28) applies. Random-walk clusters show a spectral dimension $d_s=1.14$ ($d=2$) and $d_s=1.6$ ($d=3$).[33] All the above models, however, have in common that they presumably do not adequately describe the growing process of a crystal lattice with merely orientational disorder, but they clearly indicate that the spectral dimension $d_s=1.14$ found in our experiments on DBF and the underlying fractal dimension $\bar{d}>d_s$ (although not determined in this context) are similar to those of other aggregation processes. Figure 8 may thus only serve as an illustration in case the site distribution follows randomness or diffusion-limited aggregation in the form of a ramified structure.

A final remark concerns the influence of orientational disorder on the potential energy of the DBF crystal lattice. Gavezzotti and Simonetta calculated for DBF a packing potential-energy difference $\Delta E_{\rm dis}=3.3$ kcal/mol (1150 cm^{-1}) (Ref. 34) for the two different orientations. Assuming a distribution of the two opposite orientations

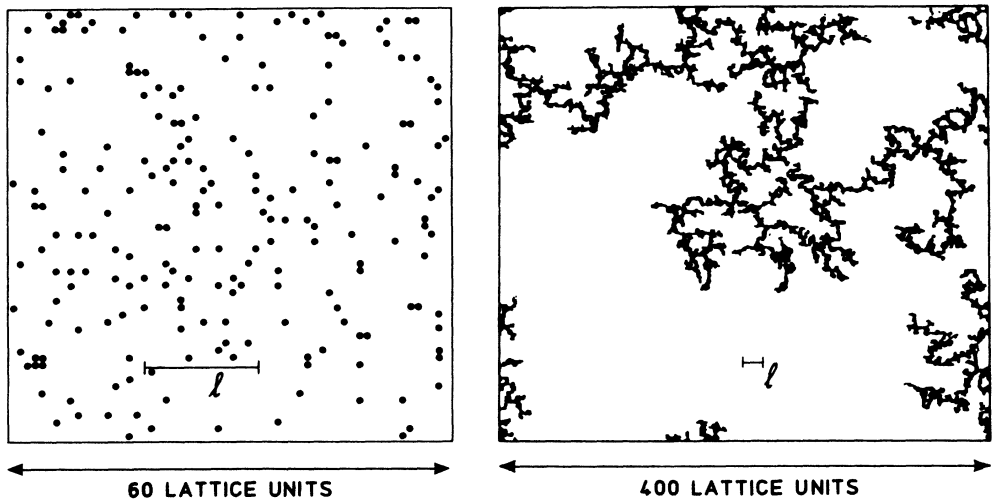

FIG. 8. Distribution of 6% (orientationally disordered) molecules on a squared lattice assuming a random distribution (left-hand side) or diffusion-limited cluster aggregation (Ref. 31) (right-hand side). The experimentally determined diffusion length $L=70$ Å is included. A random walk with length L can be easily performed on aggregated clusters, but is interrputed for a random distribution.

of DBF molecules at the solidification point at 355 K according to Boltzmann statistics, one would expect for the experimentally observed 9% misoriented molecules $\Delta E_{\text{dis}} = 1.65$ kcal/mol (575 cm^{-1}). This reduction of energy as compared to the calculated one would be easily obtained by cooperative effects such as aggregation. Comparing the crystal structure[11] and point symmetry of DBF (Fig. 1), cooperative effects are most probable in the a-b plane. This implies that two-dimensional aggregation will happen in the a-b plane, whereas three-dimensional cluster-cluster formation will follow pure statistics. Experimental work is in progress to determine additionally the fractal dimension $\bar{d}$ by doping DBF with an additional energetically lower-lying donor at low concentrations. Direct-energy transport between this donor and the low-concentrated An acceptor will, according to $I_{\text{fl}} \sim \exp(-t^{\bar{d}/s})$ (Ref. 6), explore $\bar{d}$,[35] when assuming that $s = 6$ is determined by dipole-dipole interaction responsible for the energy transport.

ACKNOWLEDGMENTS

Financial support of the Deutsche Forschungsgemeinschaft (DFG) (Sfb 337) and the Bundesministerium für Forschung und Technologie via Contract No. 313AX5C 311 is gratefully acknowledged.

[1] *Fractals in Physics,* edited by L. Pietronero and E. Tosatti (North-Holland, Amsterdam, 1986).
[2] J. S. Langer, Rev. Mod. Phys. **52**, 1 (1980).
[3] A. I. Kitaigorodsky, *Mixed Crystals* (Springer, Berlin, 1984).
[4] S. Havlin and D. Ben-Avraham, Adv. Phys. **36**, 695 (1987).
[5] G. Williams, Adv. Polym. Sci. **33**, 59 (1979).
[6] A. Blumen, J. Klafter, and G. Zumofen, in *Optical Spectroscopy of Glasses,* edited by I. Zschokke (Reidel, Dordrecht, 1986).
[7] P. Argyrakis and R. Kopelman, J. Phys. A **21**, 2753 (1988).
[8] R. Kopelman, S. Parus, and J. Prasad, Phys. Rev. Lett. **56**, 1742 (1986).
[9] C. von Borczyskowski and T. Kirski, Phys. Rev. Lett. **60**, 1578 (1988); Phys. Rev. B **40**, 11 335 (1989).
[10] H. Scher and E. W. Montroll, Phys. Rev. B **12**, 2455 (1975).
[11] W. G. Reppart, J. C. Galucci, A. P. Lundstedt, and R. E. Gerkin, Acta Crystallogr. C **40**, 1572 (1984).
[12] J. R. Morgan and M. A. El-Sayed, J. Phys. Chem. **87**, 2178 (1983).
[13] W. Schrof, R. Betz, H. Port, and H. C. Wolf, Chem. Phys. Lett. **123**, 300 (1986).
[14] U. Fischer, C. von Borczyskowski, F. Seiff, and D. Stehlik, Chem. Phys. Lett. **97**, 467 (1983).
[15] A. Bree, V. V. B. Vilkos, and R. Zwarich, J. Mol. Spectrosc. **48**, 135 (1973).
[16] A. Bree, A. R. Vacey, I. G. Ross, and R. Zwarich, Chem. Phys. Lett. **26**, 329 (1974).
[17] A. Bree, Y. H. F. Pai, and C. Taliani, Chem. Phys. Lett. **63**, 190 (1979).
[18] K. D. Hoffmann, Z. Naturforsch. Teil A **35**, 707 (1980).
[19] U. Fischer, Diploma thesis, FU Berlin, 1982; C. von Borcyskowski, U. Fischer, and D. Stehlik, Chem. Phys. Lett. **112**, 150 (1984).
[20] J. Bahrdt, P. Gürtler, and N. Schwentner, J. Chem. Phys. **86**, 6108 (1987).
[21] J. Grimm, T. Kirski, and C. von Borzyskowski, Chem. Phys. Lett. **128**, 569 (1986).
[22] R. Kohlrausch, Ann. Phys. (Leipzig) **12**, 393 (1847).
[23] H. Bässler, Phys. Status Solidi B **107**, 9 (1981).
[24] R. Richert, B. Ries, and H. Bässler, Philos. Mag. B **49**, L25 (1984); G. Peter, H. Bässler, W. Schrof, and H. Port, Chem. Phys. **94**, 445 (1985).
[25] H. Port, H. Schneckenburger, and H. C. Wolf, Z. Naturforsch. Teil A **36**, 697 (1981).
[26] A. Hammer and H. C. Wolf, Phys. Status Solidi **33**, K25 (1969).
[27] H. C. Wolf, Adv. At. Mol. Phys. **3**, 119 (1967).
[28] S. Alexander and R. Orbach, J. Phys. (Paris) Lett. **43**, L625 (1982).
[29] P. Argyrakis, in *Fractals in Physics* (Ref. 1), p. 361.
[30] D. Stauffer, *Introduction to Percolation Theory* (Taylor & Francis, London, 1985).
[31] P. Meakin, Phys. Rev. Lett. **51**, 1119 (1983).
[32] R. Jullien, M. Kolb, and R. Botet, J. Phys. Lett. **45**, L211 (1984).
[33] D. Movshovitz and S. Havlin, J. Phys. A **21**, 2761 (1988).
[34] A. Gavezzotti and M. Simonetta, in *Organic Solid State Chemistry,* edited by G. R. Desiraju (Elsevier, Amsterdam, 1987), p. 391.
[35] U. Even, K. Rademann, J. Jortner, N. Manor, and R. Reisfeld, Phys. Rev. Lett. **32**, 2164 (1984).